Cylindrical cross section optimization

Published Version:
Croccolo, D., De Agostinis, M., Fini, S., Olmi, G., Robusto, F. (2021). Cylindrical cross section optimization. PROCEEDINGS OF THE INSTITUTION OF MECHANICAL ENGINEERS. PART C, JOURNAL OF MECHANICAL ENGINEERING SCIENCE, 235(13), 2426-2436 [10.1177/0954406220953174].

Availability:
This version is available at: https://hdl.handle.net/11585/769865 since: 2026-02-13

Published:
DOI: http://doi.org/10.1177/0954406220953174

CYLINDRICAL CROSS SECTION OPTIMIZATION

D. Croccolo[a], M. De Agostinis[a], S. Fini[a], G. Olmi[a], F. Robusto[a]*

[a] Department of Industrial Engineering (DIN), University of Bologna, Viale del Risorgimento 2, 40136 Bologna, Italy

*francesco.robusto@unibo.it Tel. +39-051-2093334

Abstract: This paper focuses on cross-section optimization of both rectilinear and curvilinear beams. In particular, analytical models were developed, in order to detect how circular section resistance can be modified following a suitable cut. In fact, removing material from the furthest zone from the neutral axis, may even result in an increase of the section resistance modulus, with consequent beneficial reduction of the maximum stresses. The analytical model outcomes were confirmed by numerical analyses. This study deals with several applicative cases: in almost all of them a stress reduction was achieved, except for removing material from the extrados.

Keywords: Paradox in mechanics, section optimization, Finite Element Analysis (FEA)

List of symbols:

R: circular cross section radius	[mm]
I_{xx} : moment of inertia along the x-x axis	[mm^4]
y : distance from the x-x axis	[mm]
h : cross section height after cut	[mm]
θ : polar coordinate angle	[rad]
W : (bending resistance) section modulus	[mm^3]
R_e : external cross section radius	[mm]

R_i : internal cross section radius [mm]

Q : hollow section aspect ratio [-]

r_n : curved beam neutral radius [mm]

r_g : curved beam barycentric radius [mm]

r_{xx} : curved beam curvature radius [mm]

S_{xx} : first moment of area along the x-x axis [mm^3]

y : general coordinate for the distance from the x-x axis [mm]

y_g : barycentric distance from the x-x axis [mm]

M_f : bending moment [N·mm]

$\sigma_{\max}$: maximum bending stress [MPa]

θ_{opt} : optimal cutting angle [rad]

$\theta_{\min}$: minimum cutting angle [rad]

1. Introduction

Sometimes, it may happen that, due to the restricted amount of available space, a portion of material needs to be removed from the farthest zones from the neutral axis of mechanical components. It is known from [1], that cutting off a part of a rectilinear beam, thus reducing its cross section, may even increase its resistance section modulus. It means that, under bending moment, a reduction of maximum stress can be achieved, removing material from the cross section, although it may seem to be counterintuitive. This particular outcome is related to the definition of the inertia moment: by cutting off the corners, the moment of inertia of the cross section is lowered in a smaller proportion than the depth (maximum distance from the neutral axis); hence, the section modulus increases, and the maximum bending stress decreases.

Some other authors have dealt with this question [2]–[10], but no study was focused on hollow cross section and curvilinear beams. In particular, Strozzi et al. [11] proposed an approximated analytical approach based on Gateaux linearization. However, this analytical theory is applied to full cross section rectilinear beams only, whereas extensions to hollow cross sections rectilinear or curved are missing.

In this paper some applicative cases of hollow cross section beams, both with rectilinear and with curved geometries, are considered, thus remarkably extending the state of the art in the field. Thus, issues of novelty arise from this extension being tackled by analytical models like in [11], with numerical proof of the main results.

Motivations stem, from the possible applications of this study for design purposes, mainly aiming at a reduction of the engaged space and at weight reduction. This study can be applied to design of helical torsion springs, where the coil works under bending moment, and where the possibility of material removal could be an interesting option, due to the low amount of space being often available, and due to achieve lightweight properties. It is necessary to point out that, although stress reduction may be sometimes negligible, the space reduction could be conversely considerable, especially for curved beams like springs. Moreover, in these components, due to their curvature, the stresses do not exhibit a linear trend along the cross section. In particular, at the inner radius the stresses could be considerably higher than at the outer one. Removing material where the fibers are highly stressed may again be a paradox, but makes it possible to approach the neutral axis to the centroid one, thus leading to a stress decrease. Tackling this further paradox, with respect to the study in [11], can be regarded as a further issue of novelty.

2. Analytical formulation

Several cases were analyzed, in order to assess how, different circular cross sections are affected by material removal. As a total, 3 cases were studied, two for straight beams and one for curved ones:

- rectilinear beam
    - full circular cross section
    - hollow cross section
- curved beam
    - full circular cross section

2.1 Rectilinear beam full cross section

The analytical model was developed starting from a rectilinear beam with a circular cross section, as shown in Fig. 1, operating under constant bending moment M_f. Removing the material from both sides, the moment of inertia of the circular cross section can be written as the following:

$$I_{xx} = \int_A y^2 \cdot dA = \int_{-h}^{h} 2 \cdot R' \cdot h^2 dh \tag{1}$$

Where t is the radial material removed, $h = R - t$, θ can be defined as $\theta = \arcsin\left(\frac{R-t}{R}\right)$

$R' = R\cdot\cos\vartheta$ and $h = R\cdot\sin\vartheta$. In order to change the variable, $dh = R\cdot\cos\vartheta\cdot d\vartheta$. So, Eq. (1) can be written as:

$$I_{xx} = \int_{-\theta}^{+\theta} 2\cdot R^4\cdot\cos^2\vartheta\cdot\sin^2\vartheta\cdot d\vartheta = \frac{R^4}{8}\left[4\theta - \sin(4\theta)\right] \tag{2}$$

The section resistance moment with respect to the neutral axis is:

$$W = \frac{R^3}{8\cdot\sin\theta}\left[4\theta - \sin(4\theta)\right] \tag{3}$$

Conversely, the area of the cross-section can be written as:

$$A = \int_{-h}^{+h} 2R'\cdot dh = \int_{-\theta}^{+\theta} 2R^2\cos^2\vartheta\cdot d\vartheta = R^2\left[2\theta + \sin(2\theta)\right] \tag{4}$$

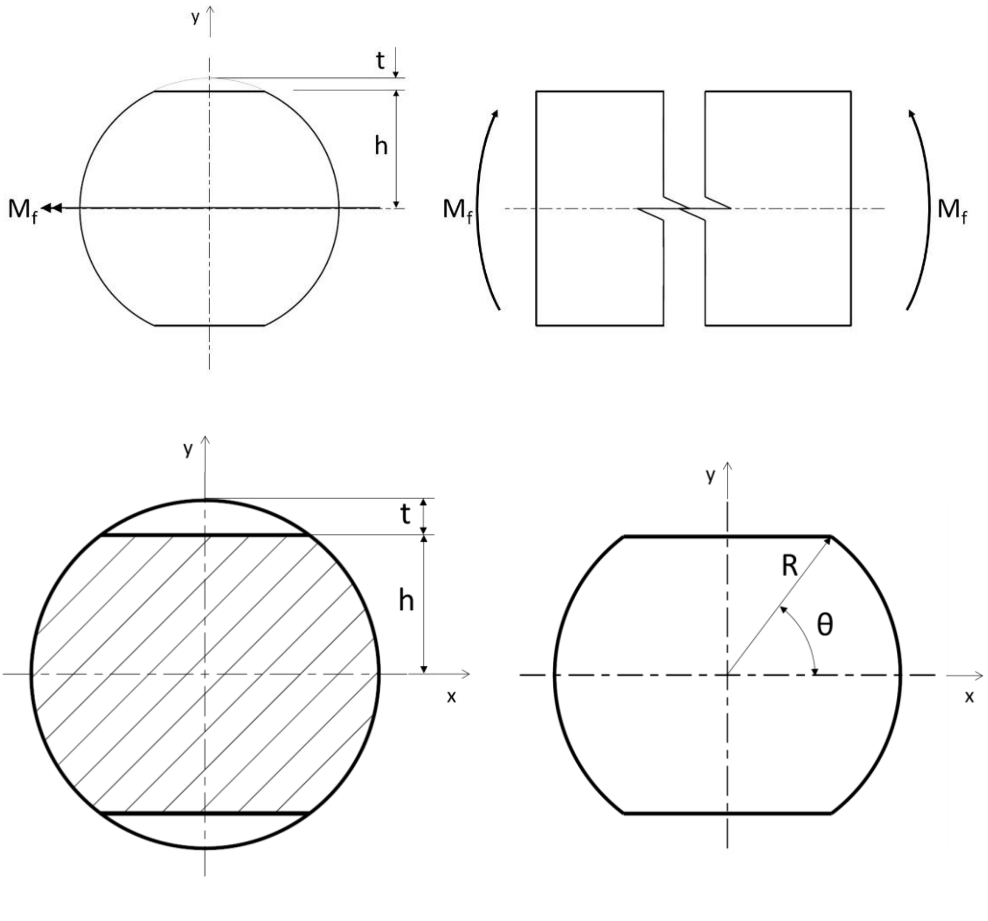

Fig. 1 – Full cross section

2.2 Rectilinear beam hollow cross section

A rectilinear beam with hollow cross section was analyzed as showed in Fig. 2. In this case the moment of inertia of the section can be written as:

$$I_{xx} = \int_{-\theta}^{+\theta} 2 \cdot R_e^{\ 4} \cdot \cos^2 \vartheta \cdot \sin^2 \vartheta \cdot d\vartheta - \frac{\pi \cdot R_i^4}{4} = \frac{R_e^{\ 4}}{8}\left[4\theta - \sin(4\theta)\right] - \frac{\pi \cdot R_i^4}{4} \tag{5}$$

If we introduce the aspect ratio of the cross section, defined as $Q = \frac{R_i}{R_e}$, the section resistance modulus with respect to the neutral axis is yielded by Eq. (6):

$$W = \frac{R_e^{\ 3}}{8 \cdot \sin\theta}\left[4\theta - \sin(4\theta) - 2 \cdot \pi \cdot Q^4\right] \tag{6}$$

Whereas the area is:

$$A = \int_{-h}^{+h} 2R' \cdot dh = \int_{-\theta}^{+\theta} 2R_e^{\ 2} \cos^2 \vartheta \cdot d\vartheta - \pi \cdot R_i = R_e^{\ 2}\left[2\theta + \sin(2\theta) - \pi \cdot Q^2\right] \tag{7}$$

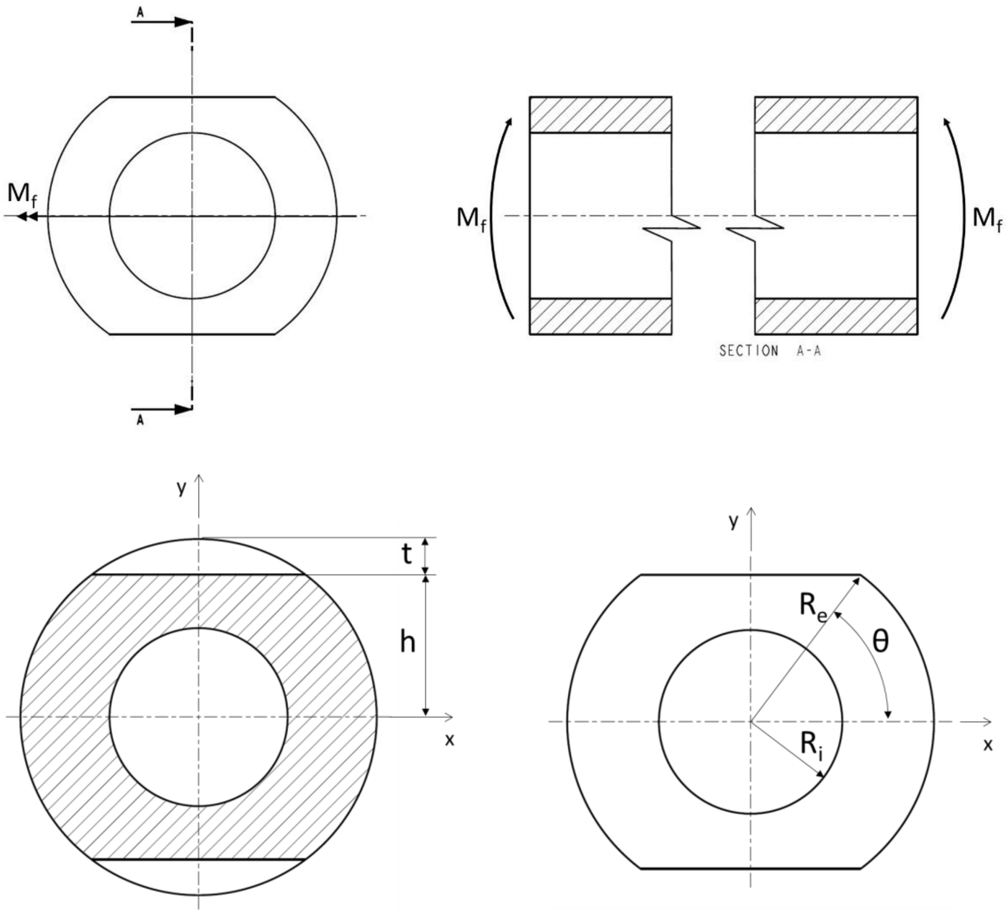

Fig. 2 – Hollow cross section

2.3 Curved beam full cross section

Full as well as hollow circular cross section curved beams are going to be analyzed here. In particular, the study was focused on how material removal from the intrados side, the extrados side or both may affect the section resistance modulus, as shown in Fig. 3. The considered geometrical parameters are reported in Fig. 4. In particular, r_{xx} represents the curvature radius of the full section and r_n the curvature at the neutral axis. The radius r_g, whereas, represent the curvature radius at the cut section center of mass.

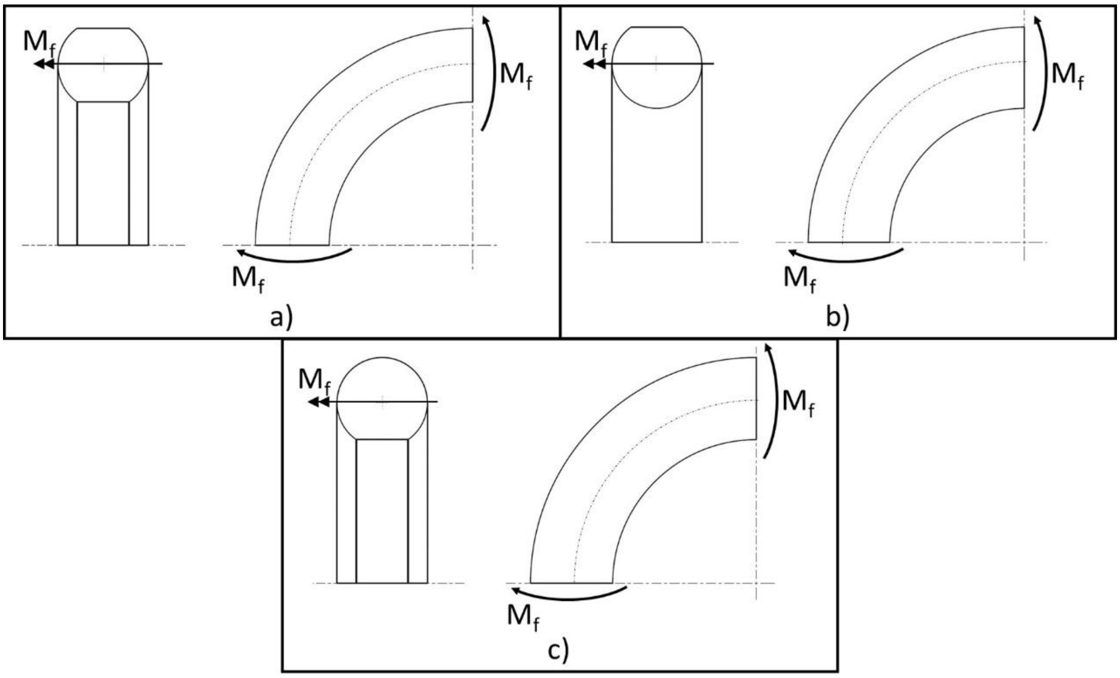

Fig. 3 – Curved beams: (a) Symmetric cutting; (b) extrados material removed; (c) intrados material removed

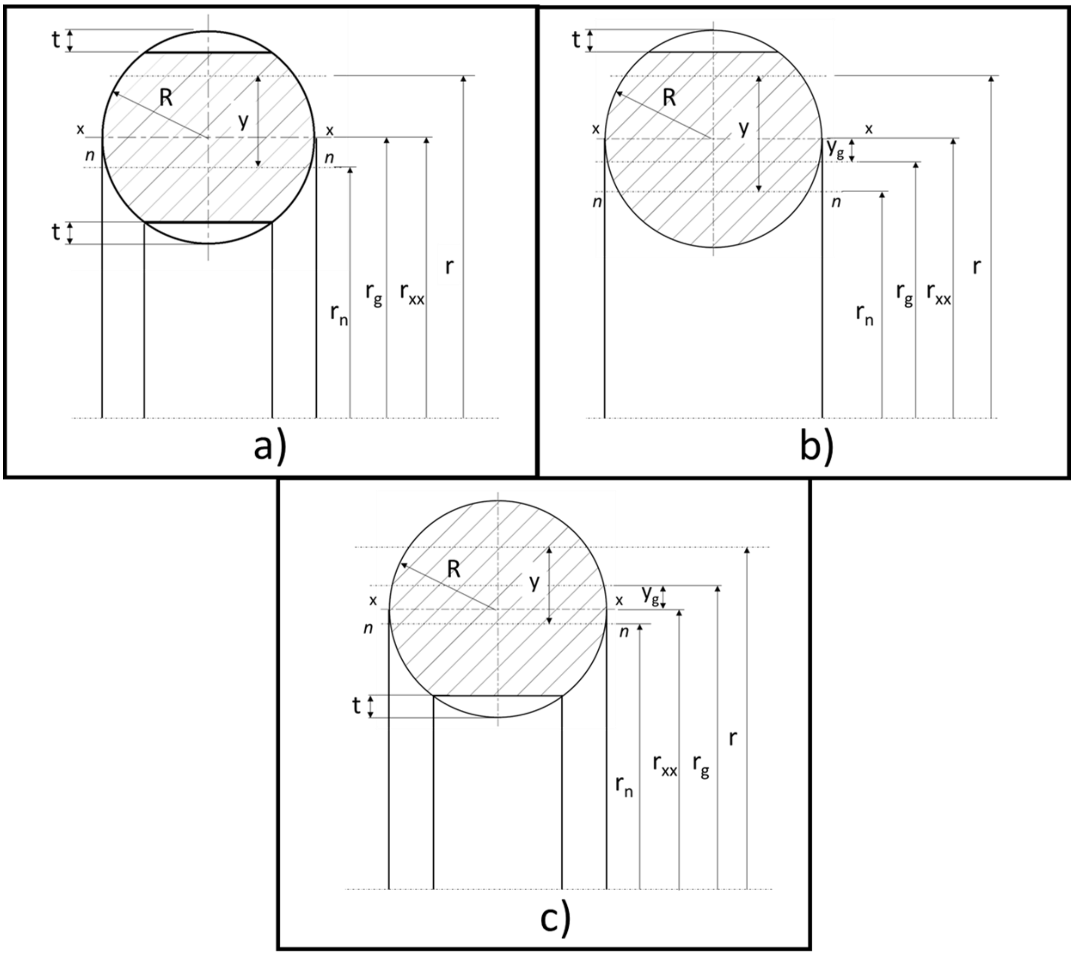

Fig. 4 – Curved beam cross section: (a) Symmetric cutting; (b) extrados material removed; (c) intrados material removed

2.3.1 Symmetric cutting

In order to obtain the section resistance modulus for a curvilinear beam, it is necessary to determine the position of the neutral axis. In the case of a symmetric cut, as sketched in Fig. 4 (a), the neutral axis can be individuated through the neutral radius r_n, as in Eq. (8):

$$r_n = \frac{A}{\int_A \frac{1}{r} dA} = \frac{\int_{-\theta}^{+\theta} 2 \cdot R^2 \cos^2 \vartheta \cdot d\vartheta}{\int_{r_{xx} - R \operatorname{Sin}\theta}^{r_{xx} + R \operatorname{Sin}\theta} \frac{2 \cdot \sqrt{R^2 - \left(r - r_{xx}\right)^2}}{r} dr} \tag{8}$$

$$= \frac{R^2 \cdot \sqrt{R^2 - r_{xx}^2} \cdot (2\theta + \sin 2\theta)}{2 \cdot \left\{ 2 \cdot r_{xx} \cdot \sqrt{R^2 - r_{xx}^2} \cdot \arctan\left(\frac{R \cdot \sin\theta}{\sqrt{R^2 \cdot \cos^2\theta}} \right) + \left(R^2 - r_{xx}^2\right) \cdot \ln\left[\frac{\left(r_{xx} + R \cdot \sin\theta\right) \cdot \left(R^2 + \sqrt{R^2 \cdot \cos^2\theta} \cdot \sqrt{R^2 - r_{xx}^2} - R \cdot r_{xx} \cdot \sin\theta\right)}{\left(r_{xx} - R \cdot \sin\theta\right)\left(R^2 + \sqrt{R^2 \cdot \cos^2\theta} \cdot \sqrt{R^2 - r_{xx}^2} + R \cdot r_{xx} \sin\theta\right)} \right] \right\}}$$

Where the term dA was evaluated according to Fig. 5.

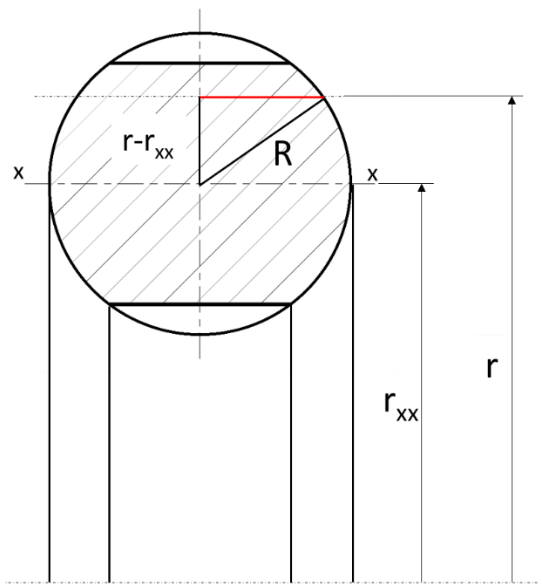

Fig. 5 – Cross section dA evaluation

The full area of the cross section is:

$$A = \int_{-h}^{+h} 2R' \cdot dh = \int_{-\theta}^{+\theta} 2R^2 \cos^2 \vartheta \cdot d\vartheta = R^2 \left[2\theta + \sin(2\theta) \right] \tag{9}$$

Due to the symmetry of the cut, the barycentric radius is unaffected and can be determined, introducing the first moment of area S_{xx}, to be equalized to zero:

$$S_{xx} = \int_A y \cdot dA = \int_{-\theta}^{\theta} 2 \cdot R^3 \cdot \mathrm{Sin}\,\vartheta \cdot \mathrm{Cos}^2\,\vartheta \cdot d\vartheta = 0 \tag{10}$$

The distance y_g of the barycenter from the axis x can be determined as in Eq. (11).

$$y_g = \frac{S_{xx}}{A} = 0 \tag{11}$$

In this case, the section resistance modulus with respect to the neutral axis can be defined as in Eq. (12):

$$|\sigma|_{\max} = \frac{M_f}{W} = \frac{M_f}{(r_g - r_n) \cdot A} \cdot \left(\frac{y}{r}\right)_{\max} \Rightarrow W = (r_g - r_n) \cdot A \cdot \left(\frac{r}{y}\right)_{\min} \tag{12}$$

Where r is the curvature of the generic radius and y is the distance of the same radius from the neutral axis.

2.3.2 Extrados cut

In this case the problem is not symmetric. The rationale for this analysis is that, when a bending moment is applied to the beam, the resulting stress distribution on the cross section is not linear. Therefore, in this section the asymmetric cut being shown in Fig. 4 (b) is analyzed. The area of the cross section is:

$$A = \int_{-R}^{+h} 2R' \cdot dh = \int_{-\frac{\pi}{2}}^{+\theta} 2R^2 \cos^2 \vartheta \cdot d\vartheta = \frac{R^2}{2}\left[\pi + 2\theta + \sin(2\theta)\right] \tag{13}$$

An important remark is that the distance between the actual barycenter of the cross section, following the extrados cut, and the geometric center of the full circular section, referenced as y_g, changes depending on the erased material. In fact, the first moment of area S_{xx} in this case is:

$$S_{xx} = \int_A y \cdot dA = \int_{-\frac{\pi}{2}}^{\theta} 2 \cdot R^3 \cdot \mathrm{Sin}\,\vartheta \cdot \mathrm{Cos}^2\,\vartheta \cdot d\vartheta = -\frac{2}{3} \cdot R^3 \cdot \mathrm{Cos}^3\,\theta \tag{14}$$

The integral in this case is not equal to zero and depends on the cutting angle θ. So, the position of the barycenter with respect to the geometrical center is:

$$y_g = \frac{S_{xx}}{A} = -\frac{4}{3} \frac{R \cdot \cos^3\theta}{\pi + 2\theta + \sin 2\theta} \tag{15}$$

Therefore, it is possible to determine the barycentric radius of the cut section as:

$$r_g = r_{xx} + y_g \tag{16}$$

It is then possible to find the neutral radius:

$$r_n = \frac{A}{\int_A \frac{1}{r} dA} = \frac{\int_{-\frac{\pi}{2}}^{\theta} 2 \cdot R^2 \cos^2\vartheta \cdot d\vartheta}{\int_{r_{xx}-R}^{r_{xx}+R\sin\theta} \frac{2 \cdot \sqrt{R^2 - (r - r_{xx})^2}}{r} dr} = \tag{17}$$

$$= \frac{R^2(\pi + 2\theta + \sin 2\theta)}{4 \cdot \left\{ r_{xx} \cdot \left[\frac{\pi}{2} + \arctan\left(\frac{R \cdot \sin\theta}{\sqrt{R^2 \cdot \cos^2\theta}} \right) \right] + \sqrt{R^2\cos^2\theta} + \sqrt{R^2 - r_{xx}^2} \cdot \ln\left[\frac{R \cdot (R - r_{xx}) \cdot (r_{xx} + R\sin\theta)}{(r_{xx} - R) \cdot \left(R^2 + \sqrt{(R^2 - r_{xx}^2) \cdot (R^2\cos^2\theta)} + R \cdot r_{xx}\sin\theta \right)} \right] \right\}}$$

The section resistance modulus can be calculated by Eq. (12).

2.3.3 Intrados cut

The section area in this case is the same as in the previous one and can be worked out by Eq. (13). The first moment of area S_{xx} in this case is:

$$S_{xx} = \int_A y \cdot dA = \int_{-\theta}^{\frac{\pi}{2}} 2 \cdot R^3 \cdot \mathrm{Sin}\,\vartheta \cdot \mathrm{Cos}^2\,\vartheta \cdot d\vartheta = \frac{2}{3} \cdot R^3 \cdot \mathrm{Cos}^3\,\theta \tag{18}$$

This means that, as an effect of material at the intrados, the barycentric radius gets increased: the position of the barycenter (of the cut section) with respect to the geometrical center (of the full section) is therefore yielded by Eq. (19):

$$y_g = \frac{S_{xx}}{A} = +\frac{4}{3} \cdot \frac{R \cdot \cos^3\theta}{\pi + 2\theta + \sin 2\theta} \tag{19}$$

Thus, it is finally possible to determine the barycentric radius of the cut section by Eq. (16).

Finally, the neutral radius is yielded by Eq. (20).

$$r_n = \frac{A}{\int_A \frac{1}{r} dA} = \frac{\int_{-\theta}^{\frac{\pi}{2}} 2 \cdot R^2 \cos^2 \vartheta \cdot d\vartheta}{\int_{r_{xx}-R\sin\theta}^{r_{xx}+R} \frac{2 \cdot \sqrt{R^2 - (r - r_{xx})^2}}{r} dr} = \tag{20}$$

$$= \frac{R^2(\pi + 2\theta + \sin 2\theta)}{2 \cdot \left\{ -r_{xx} \cdot \left[\pi + \arctan\left(\frac{R \cdot \sin\theta}{\sqrt{R^2 \cdot \cos^2\theta}} \right) \right] + \sqrt{R^2 \cos^2\theta} + \sqrt{R^2 - r_{xx}{}^2} \cdot \ln\left[\frac{R \cdot (R + r_{xx}) \cdot (r_{xx} - R\sin\theta)}{(r_{xx} + R) \cdot \left(R^2 + \sqrt{(R^2 - r_{xx}{}^2)(R^2\cos^2\theta)} - R \cdot r_{xx} \sin\theta \right)} \right] \right\}}$$

The section resistance modulus can be calculated by Eq. (12).

3. Finite element analyses

In order to confirm the analytical solutions, several FEM analyses in the elastic field were carried out by ANSYS workbench R17.1. Due to the presence of only one body, the elastic analyses are unaffected by material properties. The section resistance modulus was worked out directly from the FEM results by Eq. (21).

$$W = \frac{M_f}{|\sigma|_{\max}} \tag{21}$$

For all the analyses, the cross section was parametrized, in order to step-by-step vary the geometry of the cross section, taking the performed cut into account.

For the rectilinear FE analyses, the geometry shown in Fig. 6 was used: in particular, a rectilinear beam was used with 1 mm radius circular cross section. The beam length was set to 10 mm. A minimum mesh dimension of 0.1 mm was used. Approximately, a total of 52,000 SOLID186 elements were obtained, depending of the actual geometry of the cut section. A bending moment M_f equal to 1 Nmm was applied at one end, whereas the other one was fully constrained (clamped). In order to avoid boundary effects, considering that the de Saint Venant theory cannot be correctly applied at beam ends, maximum and minimum bending stresses were evaluated at a faraway location from the beam edges. In particular, these stresses were averaged over the 2 mm long area highlighted in Fig. 7.

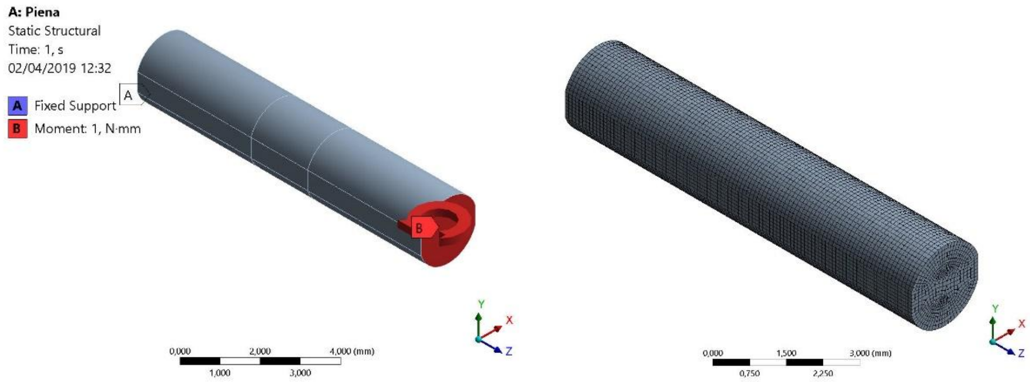

Fig. 6 – Boundary condition and mesh used for the rectilinear beam FEM analysis

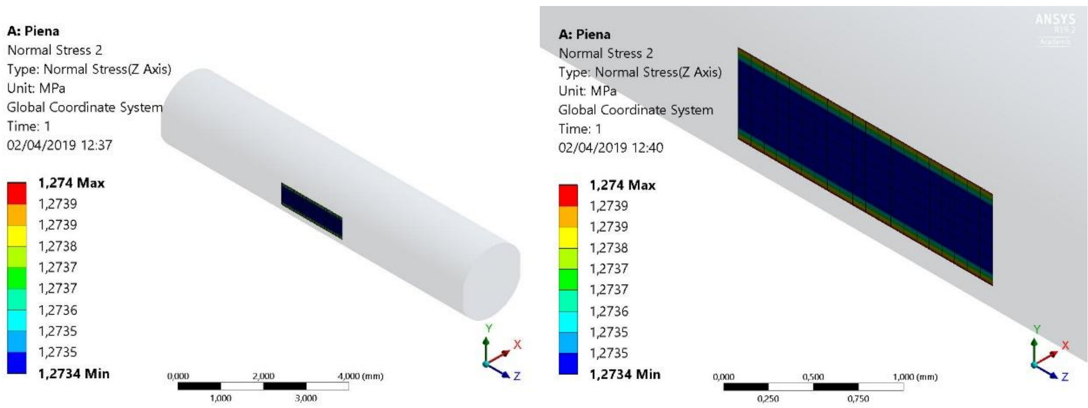

Fig. 7 – Bending stress evaluation results

When processing the curved beams, the geometry in Fig. 8 was used. For the sake of synthesis, the figures are related to the intrados cut only. A curved beam with 1 mm radius circular cross section was used, involving as well different curvature radii. A minimum mesh dimension of 0.2 mm was utilized, thus obtaining a full mesh consisting of approximately 57,000 SOLID186 elements (depending of the actual geometry of cut cross section). As above for rectilinear beams, a 1 Nmm bending moment M_f was applied at one end, whereas the other one was fully constrained. Maximum and minimum stresses were then averaged over a small area at a sufficient distance from the edges.

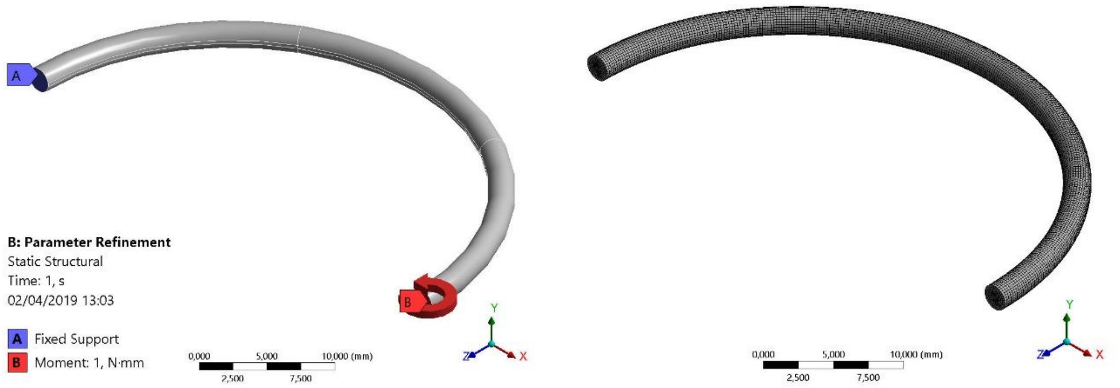

Fig. 8 – Boundary condition and mesh used for the curved beam FEM analysis

4. Results and discussion

In order to determine how the resistance modulus changes, to work out its evolution, depending on material removal, and to provide generality to the results, it is necessary to run a normalization, dividing by characteristic geometrical parameters for the investigated cases.

4.1 Rectilinear beam with cut full cross section

The resistance modulus for this geometry is plotted in Fig. 9, as a function of the cut angle, according to the analytical model. Its value is normalized by the section radius, meaning that a unitarian radius is presumed (R = 1). The same figure includes the results yiekded the FEM analyses, which are overlapped, thus highlighting an excellent agreement. It can be observed that cutting the section makes it possible to achieve a slight improvement in terms of section resistance modulus. In addition, it is possible to determine the optimal angle θ_{opt} that corresponds to the maximum resistance. Moreover, the section may also be cut accounting for an angle θ_{min} that yields the same resistance modulus of the full section, thus achieving weight reduction. These calculations can be performed with the aid of a mathematical manipulator (e.g. Wolfram Mathematica). For a rectilinear beam with full cross section the following results have been retrieved: θ_{opt} = 1.363 (78.1º) and θ_{min} = 1.254 (71.8º). Although the area reduction through the cut is negligible (1.3%), this outcome indicates the section radius may be reduced by 5%, without detrimentally affecting the section resistance, thus achieving space reduction.

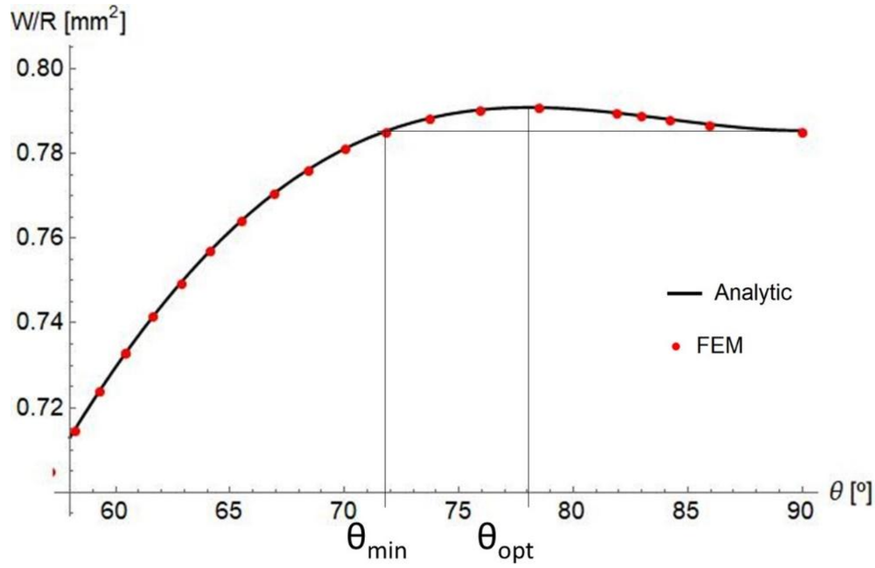

Fig. 9 – Rectilinear beam full cross section resistance modulus

4.2 Rectilinear beam hollow cross section

The results for his case were also normalized with respect to the section external radius R_e, which was posed equal to 1. The section resistance modulus, as a function of the cut angle, is plotted in Fig. 10 for different values of the aspect ratio Q.

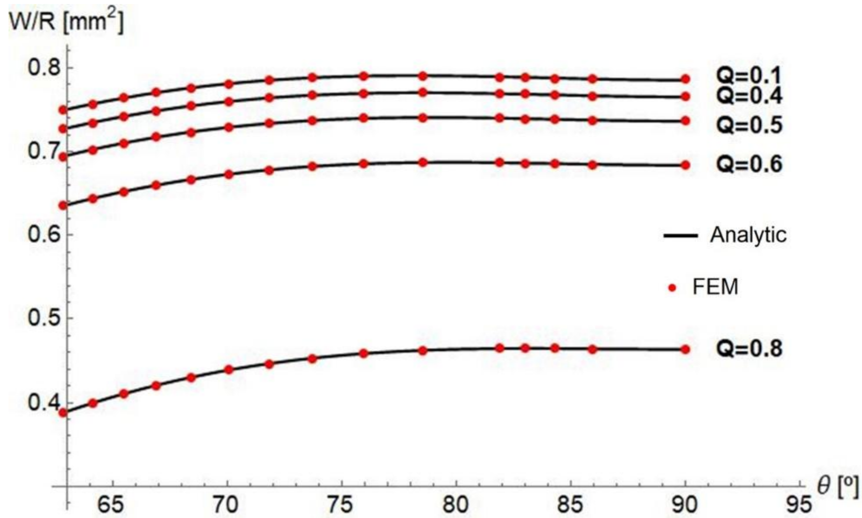

Fig. 10 - Rectilinear beam hollow cross section modulus

The θ_{min} angle introduced in the previous section has been evaluated for different values of the aspect ratio Q: it was found that, as highlighted in Fig. 11, the higher the aspect ratio, the lower the possibility of removing material from the section, without reducing its resistance modulus.

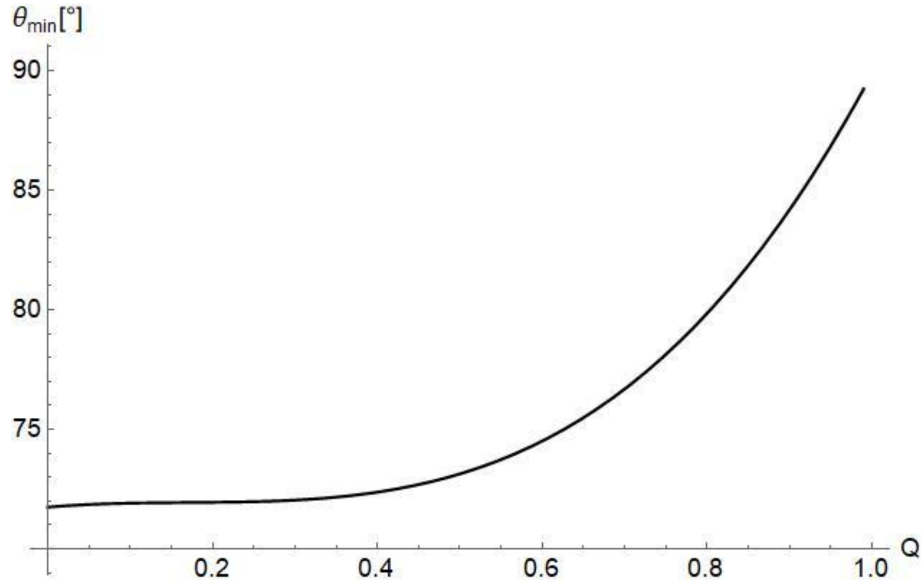

Fig. 11 - Minimum angle as a function of the aspect ratio

4.3 Curved beam with full cross section

In this section, the modulus *W* is going to be estimated, taking different values of the aspect ratio R/r_{xx} into account.

4.3.1 Symmetric cutting

When considering symmetric cuts at both sides, the maximum bending stress is always located at the intrados side. The results are shown in Fig. 12, where the bending resistance modulus is plotted versus the cut angle for a fixed value of the aforementioned aspect ratio. It can be pointed out that, for curved beams too, it proved to be safe to remove material without reducing the section modulus. In order to assess the effect of the curvature radius on the feasibility of a safe section cut, the section resistance modulus was then determined for different R/r_{xx} ratios, as shown in Fig. 13. The sketched trends indicate that, the greater the curvature (i.e.: the lower the curvature radius), the greater the feasibility of a safe and even beneficial cut. When the R/r_{xx} ratio tends to 0, which means that the curvature radius tends to infinite, the results turn to be equal to those for rectilinear beams.

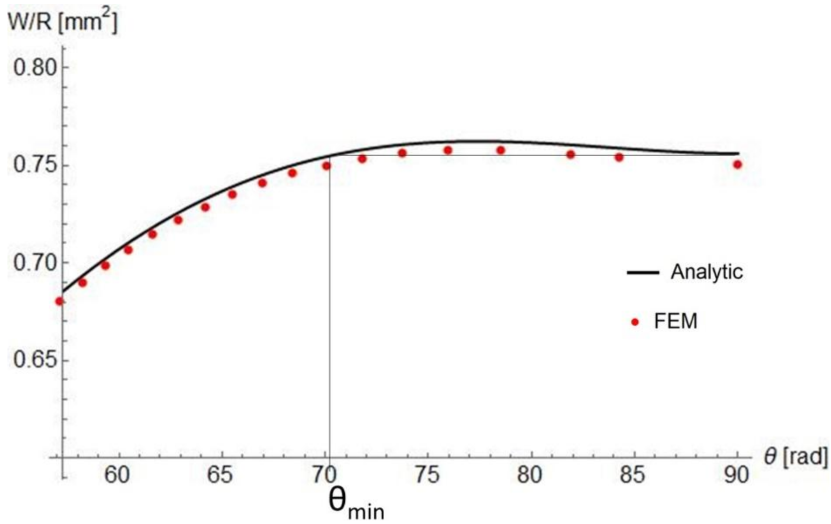

Fig. 12 – Section modulus of the section as a function of the cutting angle for R/r_{xx}=1/20.

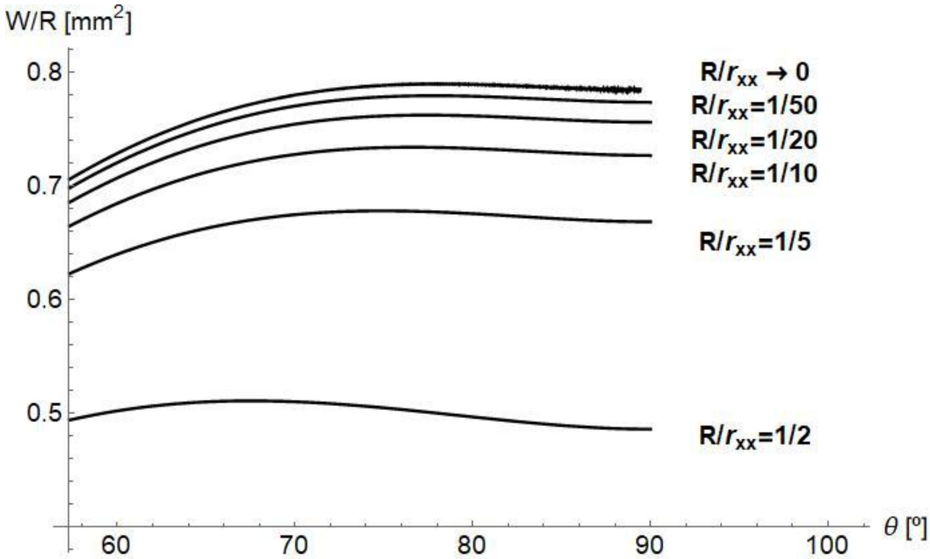

Fig. 13 – Section modulus as a function of cut angle for different values of aspect ratio (symmetric cutting)

4.3.2 Extrados cut

The bending resistance modulus is plotted in Fig. 14 for R/r_{xx}=1/20. The maximum bending stress is again always located at the intrados of the beam. However, the retrieved trend indicates that a cut at the extrados provides no improvement in terms of section modulus of the cross section: conversely, the section resistance tends to drop down. The same outcome is retrieved regardless of section proportioning, with reference to the value of R/r_{xx}, as shown in Fig. 15.

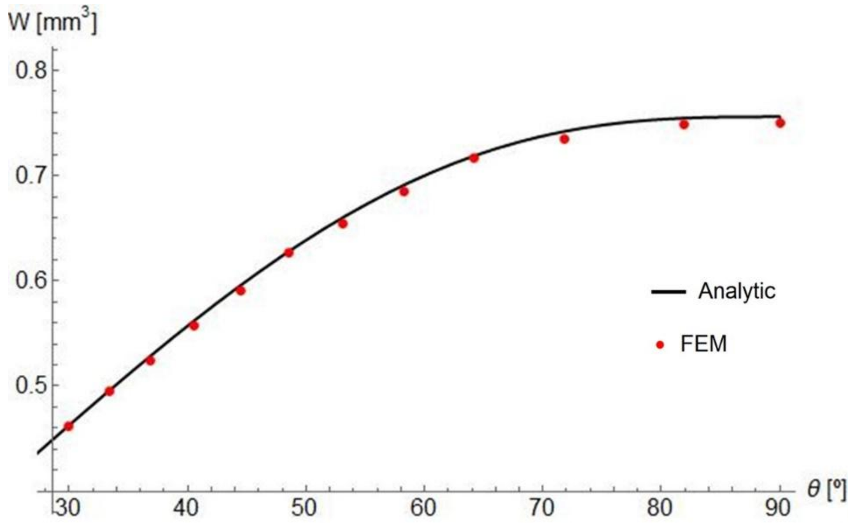

Fig. 14 – Section modulus as a function of the extrados cutting angle for $R/r_{xx}=1/20$

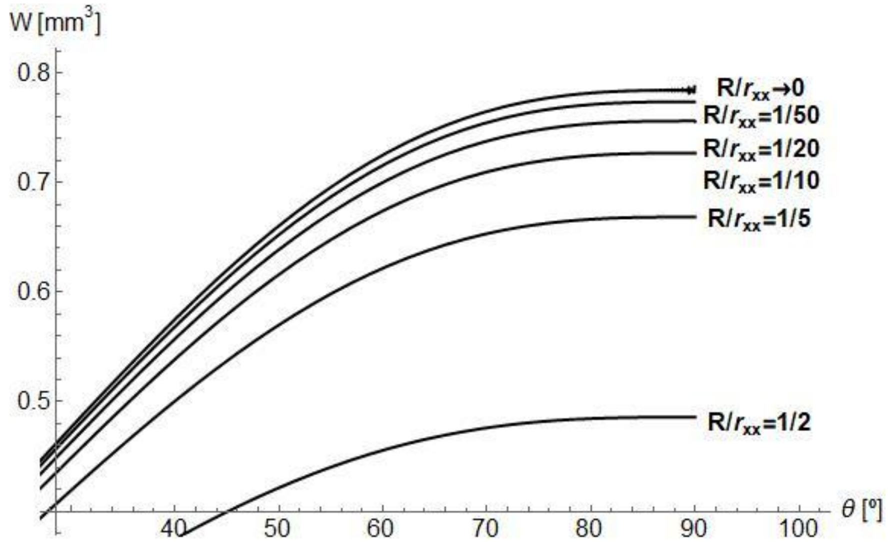

Fig. 15 – Section modulus as a function of the cutting angle plotted for different values of the aspect ratio (extrados cutting)

4.3.3 Intrados cut

The computed bending resistance modulus for this geometry is plotted in Fig. 16, for R/r_{xx}=1/20. It can be highlighted that, following a cut at the intrados, there is a range, where the section modulus gets increased. Moreover, the retrieved curve is affected by a slope discontinuity at approximately $\theta = 1.1$. This particular behavior appears to be due to the geometrical transition affecting the maximum stress location and, in turn, the maximum distance from the neutral axis. In fact, for small values of θ, the ratio in Eq. 12 between the generic radius and the distance from the neutral axis, (r/y) takes its minimum value at the extrados.

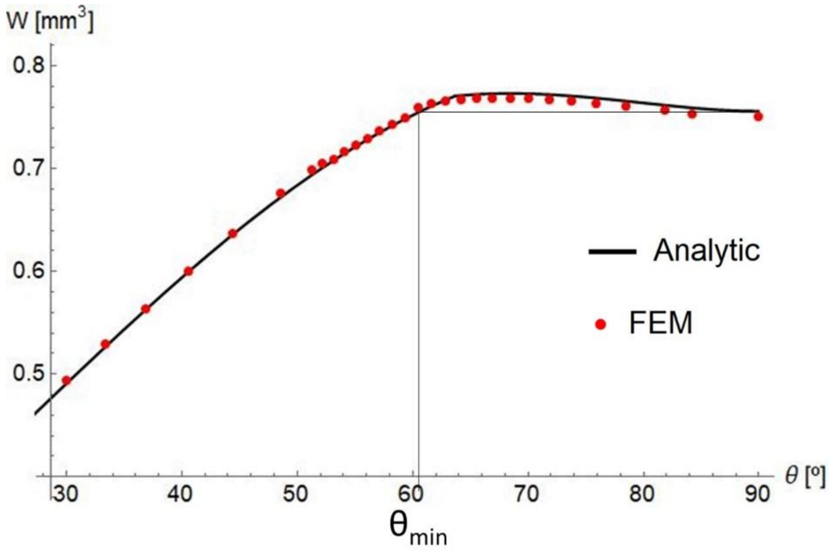

Fig. 16 - Section modulus of the section as a function of the intrados cutting angle (R/r_{xx}=1/20)

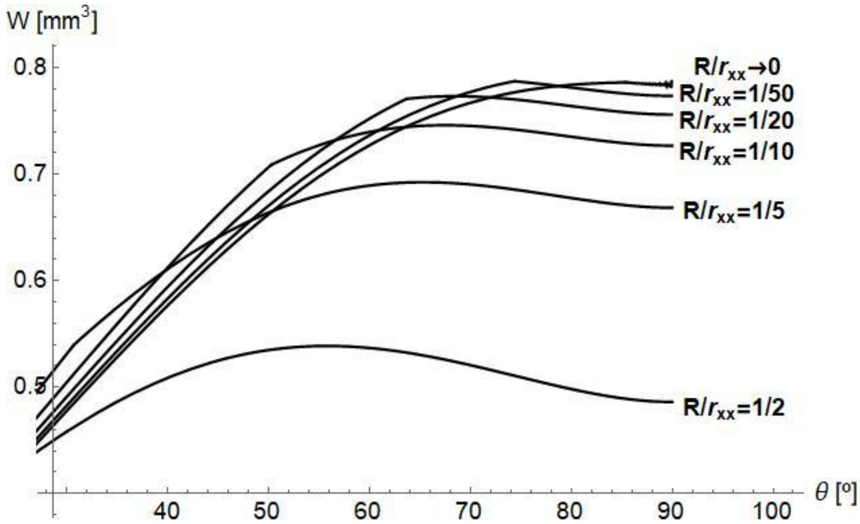

Fig. 17 – Section modulus as a function of cutting angle for different values of aspect ratio (intrados cutting)

As it can be noticed from the results plotted in Fig. 17 this behavior is more noticeable for higher values of R/r_{xx}. A possible reason is that, as the aspect ratio increases, the actual barycentric radius r_g is made more sensitive to the cut in terms of its percentage variation with respect to the curvature radius r_{xx}.

The values of the cut angle that lead to the same resistance modulus of the full cross section and are able to maximize this modulus are collected In **Errore. L'origine riferimento non è stata trovata.** for different R/r_{xx} aspect ratios on a wide range.

Table 1 – Relevant values for θ for different values of the aspect ratio

$R/r_{xx} = 1/2$	$\theta_{min} = 21.6°$	$\theta_{otp} = 55.8°$
$R/r_{xx} = 1/5$	$\theta_{min} = 41.8°$	$\theta_{otp} = 65.3°$
$R/r_{xx} = 1/10$	$\theta_{min} = 52.5°$	$\theta_{otp} = 67.5°$
$R/r_{xx} = 1/20$	$\theta_{min} = 60.7°$	$\theta_{otp} = 68.6°$
$R/r_{xx} = 1/50$	$\theta_{min} = 68.8°$	$\theta_{otp} = 74.4°$

5. Conclusions

The bending resistance modulus of circular cross section beams with added cuts, operating under pure bending loads, was analyzed in different condition. Some mathematical models were developed, to tackle this question from the analytical point of view, in order to provide generality to the results. The retrieved formulas, resumed by graphs, enable predictions on how the bending modulus is affected by section cut.

First, straight beams were studied, assessing how material removal from the furthest side of the section with respect to its neutral axis affects the section resistance. Both full and hollow cross section were studied accounting for symmetric cuts. In particular, for the latter, different aspect ratios (rations between internal and external diameters) were considered.

Secondly, curved beams were analyzed. Three different geometries were considered, accounting for material removal from both sizes, from the extrados or from the intrados only, considering as well for different proportioning ratios (ratios between the section radius and the beam curvature radius).

In order to double check the retrieved results, several FEM analyses were also carried out, involving several geometries for the cut circular sections, and determining their bending resistance moduli.

Cutting a part of a full circular cross section, when considering rectilinear beams, it is possible to achieve a resistance modulus improvement up to 0.7%. However, if diameter is decreased by a larger amount than a threshold value (5% of the total diameter), the mechanical resistance is detrimentally affected. In a hollow section rectilinear beam, a similar effect can be observed, however, the lower the aspect ratio, the higher the feasibility of fulfilling lightweight properties without worsening the section resistance.

The analysis of the curved beam with the symmetric cut shows that the cutting proves to be beneficial for the section resistance. Moreover, the higher the beam curvature, the higher the feasibility of section cutting in terms of the beneficial impact on reduced weight and/or increased resistance. The extrados cut does not lead to beneficial effects. Conversely, the intrados cut has a beneficial effect, although a slope discontinuity of the section resistance modulus can be observed in this case. This behavior can be regarded to a displacement of the section center of mass. Indeed, for lower value of θ, the ratio between the general radius and the distance from the neutral axis $(r/y)_{min}$, that appear in Eq. 12, takes its minimum value at the extrados instead of the intrados as for all other cases.

References

[1] S. Timoshenko, *Strength of Materials*. New York: John Wiley & Sons, 1930.

[2] R. E. Peterson, *Stress Concentration Factors*. 1974.

[3] T. P. Jani, P. G. Biholarav, N. R. Solanki, D. J. Jivani, A. N. Rathour, and P. H.

Darji, “Weight optimization of crane hook having 8 tons load capacity by modifying cross section and comparison with various basic cross section,” *Int J Innov. Res Adv Eng*, vol. 2, pp. 160–163, 2015.

[4] J. R. Barber, *Intermediate Mechanics of Materials*, vol. 175. 2011.

[5] A. P. Boresi, R. J. Schmidt, and O. M. Sidebottom, *Advanced Mechanics of Materials*. 1993.

[6] R. D. Milne, “Applied Functional Analysis: An Introductory Treatment,” *Appl. Funct. Anal.*, 1980.

[7] J. B. Heide and A. M. Weiss, “Vendor consideration and switching behavior for buyers in high-technology markets,” *J. Mark.*, vol. 59, no. JULY, pp. 30–43, 1995.

[8] Y. G. Panovko, *Mechanics of Deformable Solid Body: current concepts, errors, and paradoxes*. Moscow: Nauka, 1985.

[9] W. Emerson, *The principles of Mechanics*. London: James Watt, 1825.

[10] C.-L. Navier, *De la resistance des corps solides. 3 ed. avec des notes et des appendices par M. Barre de Saint-Venant.* Paris: Dunod, 1864.

[11] A. Strozzi, E. Bertocchi, and S. Mantovani, “A paradox in curved beams,” *Proc. Inst. Mech. Eng. Part C J. Mech. Eng. Sci.*, 2018.